12-20-2017

PDE8 is Expressed in Human Airway Smooth Muscle and Selectively Regulates cAMP Signaling by β 2 AR-AC6

Timothy B. Johnstone
Chapman University

Kaitlyn H. Smith
University of Tennessee Health Science Center

Cynthia J. Koziol-White
Rutgers University - New Brunswick/Piscataway

Fengying Li
University of Tennessee Health Science Center

Austin G. Kazarian
Chapman University

See next page for additional authors

Recommended Citation

Johnstone TB, Smith KH, Koziol-White CJ, et al. PDE8 is expressed in human airway smooth muscle and selectively regulates cAMP signaling by ß2AR-AC6. *Am J Respir Cell Mol Biol*. 2017. doi: 10.1165/rcmb.2017-0294OC

PDE8 is Expressed in Human Airway Smooth Muscle and Selectively Regulates cAMP Signaling by β 2 AR-AC6

Authors
Timothy B. Johnstone, Kaitlyn H. Smith, Cynthia J. Koziol-White, Fengying Li, Austin G. Kazarian, Maia L. Corpuz, Maya Shumyachter, Frederick J. Ehlert, Bianca E. Himes, Reynold A. Pannettieri Jr., and Rennolds S. Ostrom

AJRCMB Articles in Press. Published on 20-December-2017 as 10.1165/rcmb.2017-0294OC

PDE8 is expressed in human airway smooth muscle and selectively regulates cAMP signaling by ß$_2$AR-AC6

Timothy B. Johnstone[1], Kaitlyn H. Smith[2], Cynthia J. Koziol-White[4], Fengying Li[2], Austin G. Kazarian[1], Maia L. Corpuz[1], Maya Shumyatcher[3], Frederick J. Ehlert[5], Blanca E. Himes[3], Reynold A. Panettieri, Jr.[4] and Rennolds S Ostrom[1]

1. Department of Biomedical and Pharmaceutical Sciences, Chapman University School of Pharmacy, Irvine, CA
2. Department of Pharmacology, University of Tennessee Health Science Center, Memphis, TN
3. Department of Biostatistics, Epidemiology and Informatics, University of Pennsylvania, Philadelphia, PA
4. Rutgers Institute for Translational Medicine and Science, Child Health Institute, Rutgers University, New Brunswick, NJ
5. Department of Pharmacology, School of Medicine, University of California, Irvine, Irvine, CA

Running title: PDE8 regulates ß$_2$AR cAMP in airway smooth muscle

Address correspondence to: Rennolds S Ostrom, Ph.D.

Department of Biomedical and Pharmaceutical Sciences

Chapman University School of Pharmacy

9501 Jeronimo Road

Irvine, CA 92618

(714) 516-5434

FAX (714) 516-5481

rostrom@chapman.edu

Author Contributions:

Conception and design: TJ, FE, BH, RP, RO

Conducted experiments: TJ, KS, CK, FL, AK, MC, MS, BE, RO

Analysis and interpretation: TJ, KS, CK, MS, FE, BE, RP, RO

Drafting the manuscript for important intellectual content: TJ, KS, CK, FJ, BE, RP, RO

AJRCMB Articles in Press. Published on 20-December-2017 as 10.1165/rcmb.2017-0294OC

Abstract

Two cAMP signaling compartments centering around adenylyl cyclase (AC) exist in human airway smooth muscle (HASM) cells, one containing ß$_2$AR-AC6 and another containing E prostanoid receptors (EPR)-AC2. We hypothesized that different phosphodiesterase (PDE) isozymes selectively regulate cAMP signaling in each compartment. According to RNA-seq data, 18 of 24 PDE genes were expressed in primary HASM cells derived from age- and gender-matched donors with and without asthma. *PDE8A* was the third most abundant of the cAMP-degrading PDE genes, after *PDE4A* and *PDE1A*. Knockdown of PDE8A using shRNA evoked 2-fold greater cAMP responses to 1 μM forskolin in the presence of IBMX. Overexpression of AC2 did not alter this response, but overexpression of AC6 increased cAMP responses an additional 80%. We examined cAMP dynamics in live HASM cells using a fluorescent sensor. PF-04957325, a PDE8-selective inhibitor, increased basal cAMP levels by itself, indicating a significant basal level of cAMP synthesis. In the presence of an AC inhibitor to reduce basal signaling, PF-04957325 accelerated cAMP production and increased the inhibition of cell proliferation induced by isoproterenol, but had no effect on cAMP levels or cell proliferation regulated by PGE_2. Lipid raft fractionation of HASM cells revealed PDE8A immunoreactivity in buoyant fractions containing caveolin-1 and AC5/6 immunoreactivity. Thus, PDE8 is expressed in lipid rafts of HASM cells where it specifically regulates ß$_2$AR-AC6 signaling without effects on signaling by the $EP_{2/4}$R-AC2 complex. In airway diseases such as asthma and COPD, PDE8 may represent a novel therapeutic target to modulate HASM responsiveness and airway remodeling.

Introduction

Human airway smooth muscle (HASM) hypercontractility in asthma and chronic obstructive pulmonary disease (COPD) has long been managed through the use of short acting and long acting ßAR agonists. Protein kinase A (PKA) activation by cyclic adenosine monophosphate (cAMP) is a key step in bronchodilation (1), thus defining the elements responsible for cAMP signal termination is critical. Many G-protein coupled receptors (GPCR) expressed in HASM cells utilize cAMP signaling as their main second messenger, but agonists for these receptors elicit different responses. This phenomenon supports the widely held belief that cAMP signaling is compartmentalized (2, 3) yet little is known about how cells accomplish this compartmentation (4). Cells require discrete signaling elements to convey both spatial and temporal cAMP dynamics in order to selectively and finely tune propagated responses. GPCR selectively organize the initial response from paracrine, hormonal or transmitter effectors to modulate subsequent intracellular changes in cAMP levels by coupling through G_s and/or G_i proteins (5, 6). Adenylyl cyclases (AC) produce cAMP, but also assemble selective responses based on AC isoform-specific stratification to raft or non-raft microdomains, proximity to associated GPCRs and scaffolding of associated proteins and enzymes to create distinct signalosomes (4, 7). Two principle cAMP signaling compartments have been defined in HASM, one consisting of $ß_2$AR coupled to AC6 and another of EP_2 and EP_4 receptors coupled exclusively to AC2 (8-11). This cAMP "circuitry" is a dynamic and dimensional network that decodes similar, context-specific cAMP signals from different GPCRs and integrates the input for membrane, cytosolic or nuclear output targets within the cell.

Phosphodiesterases (PDE) terminate cAMP signals by catalyzing the conversion of cAMP into 5'-AMP and regulate the duration and magnitude of signaling at localized complexes to provide spatial regulation (12). These properties confer a distinct role for PDEs to sculpt the circuitry by shaping the strength and intracellular direction of the cAMP signal (3). PDEs influence signal gain, or sensitivity of output relative to degree of input. PDEs also regulate

AJRCMB Articles in Press. Published on 20-December-2017 as 10.1165/rcmb.2017-0294OC

sensitivity of cAMP pathways by participating as negative feedback regulators of cell signaling since PDE upregulation ensures that additional signaling won't produce a cellular response until a higher stimulus threshold is reached (13-15). A-kinase anchoring proteins (AKAP) play a central role in tethering PKA to PDE in order to facilitate this negative feedback (16). PDEs constitute a superfamily of 24 genes that are classified into eleven gene families (PDE1 to PDE11) according to their N-terminal domains. Different cell types orchestrate PDE activity in cells by expressing a unique complement of PDE genes depending on the spatial and kinetic requirements for cAMP signaling (12). Thus, the potential to selectively modulate cAMP signaling at the PDE level is significant but little is known about how different PDE isozymes localize to cAMP signalosomes (2, 3).

Inhibition of PDE4 augments β-agonist relaxation of smooth muscle cells and promote bronchodilation (17, 18). However, PDE4 control exerted over ßAR signaling appears to be broad (19). PDE4 inhibitors have non-selective and indiscriminate effects in many tissues, limiting their therapeutic utility (20, 21). PDE8 may selectively modulate $ß_2$AR signaling with fewer side effects: it has higher affinity and lower K_m for cAMP than other PDE isoforms in order to shape low-level, highly localized cAMP signals (22, 23). Cardiac myocytes of *PDE8A* knockout mice display higher Ca^{2+} transients, greater basal Ca^{2+} spark frequency and increased LTCC current after isoproterenol stimulation (24). These reflect changes in basal settings that occur without induction of global PKA activity and may indicate compartment specific control by PDE8.

The present study sought to define the PDE isozymes expressed in HASM cells, with the goal of determining if specific PDEs participate in previously defined cAMP signaling compartments (8, 10). Our studies indicate that a less widely expressed isoform of PDE, *PDE8A*, is expressed in HASM cells. We present a possible role of PDE8 in these cells using specific PDE8 inhibitors and shRNA knockdown of PDE8A expression. Our findings are consistent with the idea that PDE8A localizes in lipid raft microdomains where its activity shapes

responses to colocalized ß$_2$AR-AC6 signals without altering AC2 signaling by EPR localized in non-raft microdomains.

Some of the results of these studies have been previously reported in the form of an abstract (25).

Materials and Methods

Materials: Forskolin was purchased from LC Laboratories (Woburn, MA). PF-04957325 was a generous gift from Pfizer, Inc. Cell culture media and components were purchased from ThermoFisher (Waltham, MA). Fetal bovine serum was purchased from Atlanta Biologicals (Flowery Branch, GA). Lentiviral particles expressing PDE8A shRNA were purchased from Santa Cruz Biotechnology (Dallas, TX). Secondary antibodies were obtained from Santa Cruz Biotechnology. All other drugs and chemicals were purchased from Sigma Aldrich (St Louis, MO) unless otherwise noted.

Cell culture: HASM cells were isolated from deceased, de-identified lung donors by enzymatic dissociation in accordance with Institutional Review Board approval and as described previously (26). HASM cells were grown in Ham's F-12 media supplemented with 10% fetal bovine serum, pen/strep, 25 mM HEPES, 1.7 mM $CaCl_2$, and L-glutamine. Cells were kept at 5% CO_2 and 37° C. Experiments were performed on cells from passage 3-7 using over 20 different primary cell isolates in total, and at least 3 different isolates for each study. Adenoviral constructs expressing AC2, AC6, or lacZ (control) cDNA were used in AC overexpression studies. The titer of AC virus was chosen to give similar global cAMP levels in response to 1 μM forskolin. Cells were infected 18 h before treatment.

RNA-Seq: We obtained RNA-Seq results from previously published study for transcripts of all known PDE genes (27). Briefly, primary ASM cells were isolated from ten white non-smoking donors with no chronic illness or medication use and from five white asthmatic donors.

AJRCMB Articles in Press. Published on 20-December-2017 as 10.1165/rcmb.2017-0294OC

ASM cell cultivation was described previously (26, 28). Passages 4 to 7 ASM cells maintained in Ham's F12 medium supplemented with 10% FBS, $CaCl_2$, buffered with HEPES, penicillin/streptomycin, primocin, and additional L-glutamine were used in all experiments. The F12 medium was used for culture because it provides Ca^{2+} levels that are consistent with seeing contractility of muscles in that media. Total RNA was extracted from cells using the miRNAeasy mini kit (Qiagen Sciences, Inc., Germantown, MD). Approximately 1 μg of RNA from each sample was used to generate RNA-Seq cDNA libraries for sequencing using the TruSeq RNA Sample Prep Kit v2 (Illumina, Inc., San Diego, CA). Sequencing of 75 bp paired-end reads was performed with an Illumina HiSeq 2000 instrument at Partners Personalized Medicine (Boston, MA). Taffeta scripts (https://github.com/blancahimes/taffeta) were used to analyze RNA-Seq data, which included trimming of adapters using trimmomatic (v.0.32) (29) and using FastQC (v.0.11.2, Babraham Bioinformatics) to obtain overall QC metrics. Kallisto software was used to estimate transcript counts according to the hg38 Ensembl reference human genome (30). Sleuth software was used to test for differential expression of transcripts between asthma and non-asthma donors (31). Transcripts were considered to be expressed if at least 47% of samples had 5 or more reads. Plots were made with R software*. RNA-Seq data is available in the Gene Expression Omnibus (GEO) under accession GSE58434.

cAMP assays: For endpoint studies, HASM cells were grown to 80% confluency on 24-well plates, washed once with serum- and $NaHCO_3$-free Dulbecco's Modified Eagle's medium (DMEM) supplemented with 20 mM HEPES, pH 7.4 (DMEH) then equilibrated for 30 min in a 37℃ water bath. In most studies, cells were pretreated with 0.2 mM IBMX (a broad spectrum PDE inhibitor) then exposed to the indicated drug for 15 min. In other studies, no IBMX was included and the assay incubation time was 7 min. Assay medium was aspirated at the end of the incubation period and 30 μL lysis buffer was added to each well to terminate the reaction. cAMP content was then assayed using the HitHunter cAMP Assay for Small Molecules Kit

(DiscoverX, Freemont, CA). Data was normalized to the average amount of total protein on each plate, as determined using a dye binding protein assay (Bio-Rad, Hercules, CA).

For kinetic measurement of cAMP production in live cells, subconfluent HASM cells were plated on a black-walled, clear flat bottom 96-well plate with 100 µL of HASM cell media, 40 µL of BacMam virus expressing the green cAMP difference detector in situ (cADDis) cAMP sensor (Montana Molecular, Bozeman, MT), and 1 µM trichostatin-A (Sigma Aldrich, St. Louis, MO) per well. Cells were grown overnight at 5% CO_2 and 37 °C. Media was aspirated and replaced with 180 µL per well of 1X Dulbecco's Phosphate Buffered Saline Solution without calcium and magnesium. The 96-well plate was covered with aluminum foil and incubated at RT for 30 minutes. Cell fluorescence was read from the plate bottom using excitation/emission wavelengths of 494 nm and 522 nm, respectively, using a SpectraMax M5 plate reader (Molecular Devices, Sunnyvale, CA). A 5 minute kinetic read on unstimulated cells was performed to determine the variability in each well's fluorescence was ≤5%. Cells were stimulated with agonist and/or PDE inhibitor and fluorescence changes in each well were read at 30 second intervals for 30 minutes. Data were fit to a single site decay model using Graphpad Prism 6.0h (GraphPad Software Inc., San Diego, CA). In some cases, the kinetic rate constant, k, was compared between treatments by constraining the curve fits to a common plateau and plotting k to compare the rate of cAMP production across different treatments.

For assays of adenylyl cyclase activity, membranes from HASM cells were prepared by scraping cells into a hypotonic homogenizing buffer (30 mM Na-HEPES, 5 mM $MgCl_2$, 1 mM EGTA, 2 mM DTT, pH 7.5) and homogenizing in a Dounce homogenizer. The homogenate was spun at 300g for 5 min at 4˚C then transferred to a new tube and spun at 5,000g for 10 min. The pellet was suspended in membrane buffer (30 mM Na-HEPES, 5 mM $MgCl_2$, 2 mM DTT, pH 7.5) to yeild 1 mg/ml total protein concentration. 30 µl of membranes were added to assay buffer (30 mM Na-HEPES, 100 mM NaCl, 1 mM EGTA, 10 mM $MgCl_2$, 1 mM isobutylmethylxanthine, 1 mM ATP, 10 mM phosphocreatine, 5µM GTP, 60 U/ml creatine

AJRCMB Articles in Press. Published on 20-December-2017 as 10.1165/rcmb.2017-0294OC

phosphokinase and 0.1% bovine serum albumin, pH 7.5.) and either 1 μM forskolin or 10 μM SQ22536 or both. Reactions were rn for 15 min at 30˚C then were stopped by boiling for 5 min. cAMP content of each tube was assayed for cAMP content using the HitHunter cAMP Assay for Small Molecules Kit (DiscoverX, Fremont, CA). Total protein concentration was determined using a dye-binding protein assay (Bio-Rad).

Non-detergent isolation of lipid raft and non-raft membranes: Cells were fractionated using a detergent-free method as previously described (8). HASM cells were grown to 70 to 80% confluency on 10-cm plates. Cells were washed twice in ice-cold PBS, scraped off the plate in 500 mM sodium carbonate, pH 11, then homogenized with 20 strokes in a glass-glass tissue grinder followed by three 20 second bursts with an ultrasonic cell disruptor. An equal volume of 90% sucrose in MBS (25 mM MES and 150 mM NaCl, pH 6.5) was added. The sample was loaded at the bottom of a discontinuous sucrose gradient of 35% and 5% sucrose (prepared in MBS with 250 mM Na_2CO_3). The gradient was centrifuged at 46,000 rpm on a SW55Ti rotor (Beckman Coulter, Brea, CA) for 18 h at 4°C. 500 mL fractions were collected from the top of the gradient and then analyzed by SDS-PAGE (loading equal proportions of each fraction) and immunoblotting. For AC isoform detection, samples were deglycosylated and concentrated prior to SDS-PAGE. 80-100 μg protein was incubated with PNG-F in 60 mM NaCl, 1.25 mM EDTA, 143 mM ß-mercaptoethanol, 5 mM sodium phosphate, 15 mM Tris-Cl (pH 7.5), 0.1% SDS, and 0.5% Nonidet P-40 for 2 h at 37 °C. Reactions were terminated with 0.33 volumes of 4x SDS-PAGE sample buffer.

Immunoblot analysis: Whole cell lysates were obtained by scraping cells in modified RIPA lysis buffer (50 mM Tris-HCl, pH 7.5, 150 mM NaCl, 1% Igepal CA-630, plus mammalian protease inhibitor cocktail, Sigma Aldrich cat# P-8340) and homogenizing by sonication. Whole cell lysates or cell fractions were separated on 10% SDS-polyacrylamide gels by electrophoresis before being transferred to PVDF membranes (Millipore, Billerica, MA) by electroblotting. Membranes were blocked in 20 mM phosphate buffered saline (PBS) with 3%

nonfat dry milk and incubated with primary antibody 2-12 h at 4°C with constant rocking. PDE8A antibody (sc-17232, 1:200 dilution), ß-actin antibody (sc-47778, 1:1000 dilution), AC2 antibody (sc-587, 1:200 dilution) and AC5/6 antibody (sc-590, 1:200 dilution) were obtained from Santa Cruz Biotechnology (Dallas, TX). Caveolin-1 monoclonal antibody (610057, 1:1000 dilution) was obtained from BD Biosciences (San Jose, CA). Bound primary antibodies were visualized using appropriate secondary antibody with conjugated horseradish peroxidase (Santa Cruz Biotechnology, Dallas TX) and ECL reagent (ThermoFisher (Waltham, MA). Images were captured using a BioRad Gel Doc system then the alignment, exposure and contrast of each image was optimized using Adobe Photoshop CS4. In some cases, immunoreactive bands were analyzed by densitometric analysis using the volume plus density method and normalized to ß-actin.

Cell proliferation assay: HASM cells were plated on 96-well plates at a density of 5000 cells per well. After attachment, media was changed to serum free conditions (Ham's F-12 supplemented with 1% insulin-transferrin-selenium (Sigma-Aldrich), pen/strep, 25 mM HEPES, 1.7 mM $CaCl_2$, and L-glutamine). After 48 h the indicated drugs with or without 10% fetal bovine serum was added. After another 48 h the total cell content of each well was measured using CyQUANT NF (Thermo Fisher) according to the manufacturer's instructions.

Data analysis and Statistics: Standard curves were fit and unknown values extrapolated using GraphPad Prism 6.0h (GraphPad Software Inc., San Diego, CA). Data are presented as the mean ± SEM. Statistical comparisons (t-tests and one-way analysis of variance) were performed and graphics were generated using GraphPad Prism 6.0h (GraphPad Software Inc., San Diego, CA).

Results

In order to understand how cAMP signaling is regulated in HASM cells, we characterized the isozymes responsible for cAMP catabolism. Transcript levels for all PDE genes were

AJRCMB Articles in Press. Published on 20-December-2017 as 10.1165/rcmb.2017-0294OC

measured in HASM cells derived from age- and gender-matched donors with and without asthma using RNA-Seq. Fifty-five transcripts corresponding to 18 different PDE genes were expressed, while 6 PDE genes (i.e., *PDE1B, PDE2A, PDE6A, PDE6C, PDE6G, PDE6H*) did not have expressed transcripts (Table 1). Boxplots showing expression levels in asthma vs. non-asthma donor-derived cells for the 12 most abundant PDE gene transcripts are shown in Figure 1. None of the transcripts were differentially expressed between asthma and non-asthma donors according to false-discovery rate corrected statistics, although *PDE4A* had nominally significant results for its most abundant transcript (ENST00000380702; p=0.034). Among the PDE isoforms that hydrolyze cAMP, *PDE8A* was the third most abundant transcript (following *PDE1A* and *PDE4A* and roughly equivalent to *PDE7A*, Table 1). No previous reports have demonstrated expression of this PDE isoform in lung tissue or smooth muscle cells of any origin.

PDE8A is an IBMX-insensitive isoform that is not widely expressed in peripheral cell and tissues. Since PDE8 is not inhibited by most broad spectrum PDE inhibitors (32), we wondered if previous studies of cAMP signaling in HASM have failed to account for activity of this phosphodiesterase. We measured cAMP production in HASM cells from normal donors in the presence of 0.2 mM IBMX (to reduce activity by most other PDE isoforms) with and without dipyridamole, a PDE5/PDE8 inhibitor (22, 32-34). Basal cAMP production in lacZ controls showed no increase in cAMP production when using 30 μM dipyridamole compared to vehicle control (Figure 2A). We also overexpressed either AC2 or AC6, two isoforms natively expressed in HASM (8), to determine if increased cAMP synthesis revealed a role for PDE8A activity in either the AC2 or AC6 signaling compartments. Dipyridamole had no effect on basal cAMP levels in AC2 overexpressing HASM cells, but a small, non-significant increase in basal cAMP production was evident in AC6 overexpressing cells. When cells were stimulated with 1 μM forskolin, we observed a significant increase in cAMP levels in AC6-overexpressing HASM cells, but no significant effect in the lacZ or AC2 overexpressing cells (Figure 2B).

Dipyridamole has been reported to also inhibit MRP4, a transport channel that pumps cAMP out of cells (35). The changes we observed in Figure 2 may be confounded by altered cAMP export because this assay detected only intracellular cAMP. To attain a more specific reduction in PDE8A activity, we used shRNA to knockdown its expression. We tested a commercially available PDE8A shRNA lentiviral vector at different viral titers and treatment times to determine the optimal conditions for knockdown of PDE8A. We detected a maximum reduction in PDE8A immunoreactivity in lacZ (control), AC2- and AC6-overexpressing HASM cells (Figure 3A and 3B) four days following infection with PDE8A shRNA lentivirus. In the presence of IBMX, basal cAMP production was not significantly different between HASM cells infected with scrambled (control) lentivirus and those infected with PDE8A shRNA (Figure 3C). However, when AC activity was stimulated with 1 μM forskolin, PDE8A knockdown increased cAMP accumulation in control HASM and cells overexpressing AC6 (Figure 3D). By contrast, PDE8A knockdown did not significantly increase cAMP accumulation in HASM cells overexpressing AC2 (Figure 3D).

We next measured cAMP production across a range of forskolin concentrations. The concentration-response curves to forskolin in the absence and presence of PDE8A knockdown were superimposable in AC2-overexpressing HASM cells (Figure 3E). In AC6-overexpressing HASM cells, both the EC_{50} and E_{max} of forskolin-stimulated cAMP production were enhanced in PDE8A knockdown cells (Figure 3F). These data are consistent with the idea that PDE8A catalyzes the degradation of cAMP in the AC6 compartment with little effect on cAMP synthesized by AC2.

$ß_2$AR can couple primarily to AC6 while $EP_{2/4}$R couples to only AC2 due to the colocalization of these GPCR with their respective AC isoforms (9). We hypothesized that $ß_2$AR-mediated signaling in HASM cells is selectively regulated by PDE8A activity. To test this idea, we examined cAMP production using cADDis, a fluorescent sensor that detects cytosolic cAMP levels in live cells (36). Preliminary studies demonstrated that we could observe large

AJRCMB Articles in Press. Published on 20-December-2017 as 10.1165/rcmb.2017-0294OC

decreases in fluorescence of the downward cADDis sensor in response to various concentrations of forskolin without the addition of IBMX or other PDE inhibitors (Figure 4A). Addition of PF-04957325, a PDE8 selective inhibitor (37), also increased levels of cAMP in a concentration-dependent manner (Figure 4B and 4E). We observed a similar response with the addition of rolipram, a PDE4 selective inhibitor (Figure 4C), implying that a low level of basal AC activity exists in HASM cells. This basal AC activity is sufficient to allow PDE inhibition alone to induce cAMP responses detected by the cADDis sensor.

In order to use PF-04957325 to probe for the role of PDE8 in regulating cAMP stimulated by isoproterenol or PGE_2, this basal AC activity must be reduced. This is a critical element, since the source of the basal stimulus, and what compartment(s) and AC isoform(s) it emanates from, is unknown. We sought an established AC inhibitor that is relatively non-selective across AC isoforms. We tested several concentrations of the AC inhibitor, SQ22536 (38), to find the minimally effective concentration that reduced the cAMP response to PF-04957325 alone. 10 μM SQ22536 caused a significant reduction in the responses observed to PF-04957325 (Figure 4D and 4E). This same concentration of SQ22536 reduced AC activity in isolated HASM membranes by approximately 50% (Figure 4D inset). Using 10 μM SQ22536 to suppress basal AC activity, various concentrations of isoproterenol or PGE_2 were used to identify concentrations of each agonist that induced small but reproducible cAMP stimuli of equal magnitude. 1 nM isoproterenol or 3 nM PGE_2, which elicit half-maximal responses by the cADDis sensor when tested alone, gave ~5-10% reduction of the fluorescence signal in the presence of 10 μM SQ22536 (Figure 5A). We then measured the responses to various concentrations of PF-04957325 in the presence of 10 μM SQ22536 with either isoproterenol or PGE_2 present to provide compartment-specific stimuli. PF-04957325 increased 1 nM isoproterenol-stimulated cAMP responses in a concentration-dependent manner (Figure 5B and 5D). PF-04957325 effects on the rate of isoproterenol-stimulated cAMP production (expressed as the rate constant, k, of the fluorescent decay of the cADDis sensor) appeared to have both

low affinity and high affinity components (Figure 5D, black bars). The decrease in cAMP levels at 10nM PF-04957325 may be due to PKA-mediated phosphorylation of PDE8 that enhances its activity or to inhibition of other PDE isoforms by higher concentrations of PF-04957325 (37). 3 nM PGE_2-stimulated cAMP production was not enhanced by any concentration of PF-04957325 (Figure 5C and 5D). PF-04957325 did not increase cAMP signaling in conditions with preferential activation of either EP_2 receptors or EP_4 receptors (supplementary data, Figure S2). Thus, PDE8 activity specifically regulates cAMP signals generated by $ß_2$AR without significant effects on cAMP stimulated by either EP_2R or EP_4R.

Based on the fact that PDE8A selectively regulated $ß_2$AR- and AC6-mediated cAMP production, we hypothesized that it is localized in lipid raft microdomains. PDE8A has been reported in detergent resistant membranes from mural granulosa cells, but this study did not utilize sucrose density centrifugation to isolate lipid rafts (39). We used a non-detergent method followed by sucrose gradient centrifugation to isolate lipid raft fractions from control HASM cells. We have previously reported that $ß_2$AR, natively expressed AC6 and overexpressed AC6 co-localize in lipid raft domains, but that EP_2R, EP_4R and AC2 are excluded from these domains (8, 9). Immunoblot analysis of these fractions indicates that PDE8A co-localizes with natively expressed caveolin-1 and AC6 in buoyant, lipid raft fractions numbered 3-5, but not in fractions 6-10 associated with non-raft membranes and the bulk of the cellular material (Figure 6). AC2 immunoreactivity was only detected in lower fractions associated with non-lipid raft membranes and other cellular organelles. HASM cells incubated with lentivirus expressing PDE8A shRNA displayed no PDE8A immunoreactive bands near 93 kDa following fractionation. These data are consistent with the idea that PDE8A localizes in lipid raft microdomains where it selectively regulates signaling by $ß_2$AR and AC6.

$ß_2$AR agonists and other cAMP-elevating agents inhibit serum and growth factor-stimulated cell proliferation (40). We examined the effects of PF-04957325 on cell proliferation stimulated by serum. After 48 h of serum starvation, HASM cells were incubated with 10% FBS

AJRCMB Articles in Press. Published on 20-December-2017 as 10.1165/rcmb.2017-0294OC

and either PF-04957325 (1 μM), isoproterenol (1 μM) or PF-04957325 plus isoproterenol. PF-04957325, isoproterenol or the combination did not significantly alter cell proliferation in the absence of FBS (Figure 7A). FBS stimulated cell proliferation nearly 3 fold and treatment with just 1 μM isoproterenol or 1 μM PF-04957325 did not inhibit this response. We chose a sub-maximal concentration of isoproterenol for this study so that any additive effect from inhibition of PDE activity could be observed. Indeed, treatment of HASM cells with both isoproterenol and PF-04957325 significantly inhibited cell proliferation over FBS alone ($p<0.01$ by paired t-test). We also examined the effect of PGE_2 on HASM cell proliferation. 1 μM PGE_2 induced a small but significant ($p<0.05$) inhibition of FBS-stimulated cell proliferation, but adding PF-04957325 did not increase this effect (Figure 7B). Therefore, inhibition of PDE8 activity increases the ability of $ß_2$AR to regulate cell proliferation but has no effect on PGE_2-mediated regulation of cell proliferation.

Discussion

PDE8 function has been previously ascribed to roles in T-cell adhesion (37), adrenal (41, 42) and Leydig cell steroidogenesis (32, 43), heartbeat regulation (24) and lymphocyte/breast cancer chemotaxis (44, 45). We report here the transcript, protein and functional presence of PDE8 in human airway smooth muscle cells. Our transcriptomic data demonstrates the presence of all PDE isoenzymes, except PDE2, via selective expression of 18/24 PDE genes in HASM cells derived from donors with asthma and fatal asthma. Previously, studies were focused on soluble inhibitors to characterize PDE function in HASM cells (18). We hypothesized that PDE8 was functionally relevant in human airway smooth muscle cells because dipyridamole, a semiselective PDE5/8 inhibitor (22), induced small but non-significant increases in forskolin-stimulated cAMP accumulation (Figure 2A). Dipyridamole enhanced forskolin-stimulated cAMP in HASM cells overexpressing AC6, but not in cells overexpressing AC2, implying that PDE8 may selectively regulate signaling in AC6 microdomains. These initial

results with dipyridamole were supported by knockdown of *PDE8A* expression with shRNA. *PDE8A* knockdown selectively enhanced cAMP production in AC6 overexpressing cells relative to AC2 in basal and forskolin-stimulated conditions (Figure 3B and 3C). Moreover, knockdown of PDE8 expression shifts the forskolin dose response curve to a higher maximum in AC6 overexpressing cells (Figure 3E), but not when AC2 was overexpressed (Figure 3D). These results indicate that PDE8 changes the gain of local cAMP signaling so that stimulation of AC causes a proportionally stronger response in this particular cAMP microdomain.

Measuring cAMP levels in the presence of IBMX does not allow the interpretation of the relative importance of PDE8 in cAMP signaling compared to other PDE isoforms. Therefore, we sought an assay capable of sensitively detecting cAMP levels without broad PDE inhibition. Expression of the "downward" cADDis cAMP sensor allows sensitive detection of intracellular cAMP kinetics in live cells without PDE inhibition (Figure 4A and 4C; (36). We initially determined that lentiviral infection of HASM cells reduces BacMam infection and expression of the cADDis cAMP sensor. Therefore, shRNA knockdown of PDE8 is not compatible with the cADDis assay using the methods we employed. Instead, we employed the PDE8-selective inhibitor, PF-04957325 (42). PF-04957325 dose dependently enhanced the rate constant (k) for cAMP formation in the absence of any GPCR agonist or AC activator, indicating that accumulation of cAMP was accelerated. The response to PF-04957325 was concentration dependent and nearly as efficacious as forskolin (Figure 4A) and more efficacious than the response to the PDE4 inhibitor, rolipram (Figure 4C). Thus, basal cAMP signaling within HASM cells appears to be at least partly under PDE8 control.

We next examined the effect of PDE8 inhibition on small cAMP responses that were directly attributable to either isoproterenol or PGE_2. Addition of PF-04957325 increased cAMP levels in the presence of isoproterenol but had no effect (in fact slightly inhibited) responses in the presence of PGE_2 (Figure 5A and 5B). These responses were accompanied by selective changes in the rate constant (k) of cAMP formation in isoproterenol, but not PGE_2, stimulated

AJRCMB Articles in Press. Published on 20-December-2017 as 10.1165/rcmb.2017-0294OC

responses (Figure 5C). Interestingly, the effects of PF-04957325 on isoproterenol-induced response appeared to have both high affinity and low affinity components (Figures 4C and 5C). The reason for this is unknown, but might relate to PKA activation of PDE8 activity as cAMP levels increase or to inhibition of other PDE isoforms at higher concentrations of PF-04657325. Nonetheless, functionally responsive PDE8 appears in ß$_2$AR, but not EP$_2$R signaling microdomains.

We have previously established that ß$_2$AR are colocalized in lipid raft fractions with AC5/6, while AC2 is localized in non-raft fractions where it is colocalized with EP$_{2/4}$R (9). This is evident in HASM cells as well as many other cells and tissues (46, 47). We now show that PDE8A immunoreactivity is similarly localized in lipid raft fractions (PDE8 shRNA knockdown eliminated this signal, Figure 6) of HASM cells. The selective effect of PDE8 in regulating cAMP levels in the ß$_2$AR compartment is also evident at the functional level. Examination of cell proliferation regulated by both PGE$_2$ and isoproterenol with and without the PDE8-selective inhibitor makes it clear that PDE8 activity regulates signaling by ß$_2$AR receptors but has no effect on PGE$_2$-mediated signaling (Figure 7) through either EP$_2$ or EP$_4$ receptors (supplementary data, Figure S2). Taken together, our data indicate that PDE8 colocalizes with ß$_2$AR-AC6 in lipid-raft microdomains and shapes cAMP signals and cellular responses to ß$_2$AR. We speculate that PDE8 provides a highly localized, regional brake on cAMP signaling in HASM cells so that low threshold activation of signaling in this compartment is suppressed to minimize indiscriminate recruitment of downstream signaling effectors. The exact role of PDE8 and its regulation of ß$_2$AR-AC6 signaling could be to regulate cell shape, proliferation, contractility or perhaps overall responsiveness to changes in parasympathetic tone or other relevant hormones in the blood as a way to manage resting versus active metabolic demands (48, 49).

The utility of modulating PDEs for treatment of lung disorders like asthma and COPD has been extensively evaluated in clinical research and has culminated with the approval of roflumilast, a PDE4 inhibitor, for treatment of severe COPD (18). However PDE4-selective

inhibitors exhibit too narrow of a therapeutic window for wider use because of target-related GI side effects such as nausea, vomiting, diarrhea, abdominal pain and dyspepsia. Strategies to mitigate side effects have included combined PDE3/4 inhibition since PDE3 inhibition can synergize with PDE4 on lung bronchoconstriction and inflammation (50, 51). In addition to possible cardiac side effects, this particular strategy may be confounded by metabolic dysregulation leading to insulin resistance, as seen in PDE3B$^{-/-}$ knockout animals (52). Moreover, several PDE3/4 dual inhibitors in clinical development have been discontinued, indicating the potential synergy isn't sufficient to significantly widen the therapeutic window. While the concept of modulating cAMP sensitive pathways via inhibition of PDE activity remains attractive, more selective means of achieving signal control are needed (18). Perhaps modulation of PDE8 enzymes within airway smooth muscle could be a selective means for altering cellular responses associated with asthma or COPD, especially in the context of using agonists for β_2AR or other GPCR as co-therapies (53). For example, compartment-specific, basal-directed effects of PDE8 that occur in human airway smooth muscle cells could be a relevant target for subtle modulation of β_2AR-induced bronchodilation without long term desensitization, increases in smooth muscle hypertrophy or enhancement of cAMP signaling by other signals such as prostaglandins.

Our data are the first to demonstrate PDE8 expression and function in airway smooth muscle. We show it regulates cAMP signaling stimulated by ß$_2$AR but does not alter prostaglandin-stimulated cAMP levels in HASM cells. While more studies are needed to characterize the role of PDE8 in regulating human bronchodilation, it is clear that this unique PDE isoform has potential as a therapeutic target in asthma and COPD.

AJRCMB Articles in Press. Published on 20-December-2017 as 10.1165/rcmb.2017-0294OC

Acknowledgements

The authors thank Drs. Raymond Penn and Tonio Pera, Thomas Jefferson University, and Dr. Gaoyuan Cao and Brian Deeney, Rutgers University, for isolating and providing human airway smooth muscle cells. PF-04957325 was a generous gift of Pfizer, Inc.

References

1. Morgan SJ, Deshpande DA, Tiegs BC, Misior AM, Yan H, Hershfeld AV, Rich TC, Panettieri RA, An SS, Penn RB. Beta-agonist-mediated relaxation of airway smooth muscle is protein kinase a-dependent. *J Biol Chem* 2014;289(33):23065-23074.
2. Baillie GS. Compartmentalized signalling: Spatial regulation of camp by the action of compartmentalized phosphodiesterases. *FEBS J* 2009;276(7):1790-1799.
3. Houslay MD. Underpinning compartmentalised camp signalling through targeted camp breakdown. *Trends Biochem Sci* 2010;35(2):91-100.
4. Ostrom RS, Bogard AS, Gros R, Feldman RD. Choreographing the adenylyl cyclase signalosome: Sorting out the partners and the steps. *Naunyn Schmiedebergs Arch Pharmacol* 2012;385(1):5-12.
5. May DC, Ross EM, Gilman AG, Smigel MD. Reconstitution of catecholamine-stimulated adenylate cyclase activity using three purified proteins. *J Biol Chem* 1985;260(29):15829-15833.
6. Taussig R, Iniguez-Lluhi JA, Gilman AG. Inhibition of adenylyl cyclase by gi alpha. *Science* 1993;261(5118):218-221.
7. Cooper DM, Tabbasum VG. Adenylate cyclase-centred microdomains. *Biochem J* 2014;462(2):199-213.
8. Bogard AS, Xu C, Ostrom RS. Human bronchial smooth muscle cells express adenylyl cyclase isoforms 2, 4, and 6 in distinct membrane microdomains. *J Pharmacol Exp Ther* 2011;337(1):209-217.
9. Bogard AS, Adris P, Ostrom RS. Adenylyl cyclase 2 selectively couples to e prostanoid type 2 receptors, whereas adenylyl cyclase 3 is not receptor-regulated in airway smooth muscle. *J Pharmacol Exp Ther* 2012;342(2):586-595.
10. Bogard AS, Birg AV, Ostrom RS. Non-raft adenylyl cyclase 2 defines a camp signaling compartment that selectively regulates il-6 expression in airway smooth muscle cells: Differential regulation of gene expression by ac isoforms. *Naunyn Schmiedebergs Arch Pharmacol* 2013.
11. Agarwal SR, Miyashiro K, Latt H, Ostrom RS, Harvey RD. Compartmentalized camp responses to prostaglandin ep2 receptor activation in human airway smooth muscle cells. *Br J Pharmacol* 2017;174(16):2784-2796.
12. Zaccolo M. Spatial control of camp signalling in health and disease. *Curr Opin Pharmacol* 2011;11(6):649-655.
13. Manning CD, McLaughlin MM, Livi GP, Cieslinski LB, Torphy TJ, Barnette MS. Prolonged beta adrenoceptor stimulation up-regulates camp phosphodiesterase activity in human monocytes by increasing mrna and protein for phosphodiesterases 4a and 4b. *J Pharmacol Exp Ther* 1996;276(2):810-818.
14. Seybold J, Newton R, Wright L, Finney PA, Suttorp N, Barnes PJ, Adcock IM, Giembycz MA. Induction of phosphodiesterases 3b, 4a4, 4d1, 4d2, and 4d3 in jurkat t-cells and in human peripheral blood t-lymphocytes by 8-bromo-camp and gs-coupled receptor agonists. Potential role in beta2-adrenoreceptor desensitization. *J Biol Chem* 1998;273(32):20575-20588.
15. Dodge KL, Khouangsathiene S, Kapiloff MS, Mouton R, Hill EV, Houslay MD, Langeberg LK, Scott JD. Makap assembles a protein kinase a/pde4 phosphodiesterase camp signaling module. *Embo J* 2001;20(8):1921-1930.

AJRCMB Articles in Press. Published on 20-December-2017 as 10.1165/rcmb.2017-0294OC

16. Horvat SJ, Deshpande DA, Yan H, Panettieri RA, Codina J, DuBose TD, Jr., Xin W, Rich TC, Penn RB. A-kinase anchoring proteins regulate compartmentalized camp signaling in airway smooth muscle. *FASEB J* 2012;26(9):3670-3679.
17. Hu A, Nino G, Grunstein JS, Fatma S, Grunstein MM. Prolonged heterologous beta2-adrenoceptor desensitization promotes proasthmatic airway smooth muscle function via pka/erk1/2-mediated phosphodiesterase-4 induction. *Am J Physiol Lung Cell Mol Physiol* 2008;294(6):L1055-1067.
18. Page CP. Phosphodiesterase inhibitors for the treatment of asthma and chronic obstructive pulmonary disease. *Int Arch Allergy Immunol* 2014;165(3):152-164.
19. Lynch MJ, Baillie GS, Houslay MD. Camp-specific phosphodiesterase-4d5 (pde4d5) provides a paradigm for understanding the unique non-redundant roles that pde4 isoforms play in shaping compartmentalized camp cell signalling. *Biochem Soc Trans* 2007;35(Pt 5):938-941.
20. Kokkonen K, Kass DA. Nanodomain regulation of cardiac cyclic nucleotide signaling by phosphodiesterases. *Annu Rev Pharmacol Toxicol* 2017;57:455-479.
21. Maurice DH, Ke H, Ahmad F, Wang Y, Chung J, Manganiello VC. Advances in targeting cyclic nucleotide phosphodiesterases. *Nat Rev Drug Discov* 2014;13(4):290-314.
22. Soderling SH, Bayuga SJ, Beavo JA. Cloning and characterization of a camp-specific cyclic nucleotide phosphodiesterase. *Proc Natl Acad Sci U S A* 1998;95(15):8991-8996.
23. Wang H, Yan Z, Yang S, Cai J, Robinson H, Ke H. Kinetic and structural studies of phosphodiesterase-8a and implication on the inhibitor selectivity. *Biochemistry* 2008;47(48):12760-12768.
24. Patrucco E, Albergine MS, Santana LF, Beavo JA. Phosphodiesterase 8a (pde8a) regulates excitation-contraction coupling in ventricular myocytes. *J Mol Cell Cardiol* 2010;49(2):330-333.
25. Hill KM, Li F, Bogard AS, Ostrom RS. The ibmx-insensitive pde8a is expressed in human airway smooth muscle cells and selectively regulates signaling through ac6. . *FASEB J* 2016;30(1 Supplement).
26. Panettieri RA, Murray RK, DePalo LR, Yadvish PA, Kotlikoff MI. A human airway smooth muscle cell line that retains physiological responsiveness. *Am J Physiol* 1989;256(2 Pt 1):C329-335.
27. Himes BE, Koziol-White C, Johnson M, Nikolos C, Jester W, Klanderman B, Litonjua AA, Tantisira KG, Truskowski K, MacDonald K, et al. Vitamin d modulates expression of the airway smooth muscle transcriptome in fatal asthma. *PLoS One* 2015;10(7):e0134057.
28. Cooper PR, Mesaros AC, Zhang J, Christmas P, Stark CM, Douaidy K, Mittelman MA, Soberman RJ, Blair IA, Panettieri RA. 20-hete mediates ozone-induced, neutrophil-independent airway hyper-responsiveness in mice. *PLoS One* 2010;5(4):e10235.
29. Bolger AM, Lohse M, Usadel B. Trimmomatic: A flexible trimmer for illumina sequence data. *Bioinformatics* 2014;30(15):2114-2120.
30. Bray NL, Pimentel H, Melsted P, Pachter L. Near-optimal probabilistic rna-seq quantification. *Nat Biotechnol* 2016;34(5):525-527.
31. Pimentel H, Bray NL, Puente S, Melsted P, Pachter L. Differential analysis of rna-seq incorporating quantification uncertainty. *Nat Methods* 2017;14(7):687-690.

32. Vasta V, Shimizu-Albergine M, Beavo JA. Modulation of leydig cell function by cyclic nucleotide phosphodiesterase 8a. *Proc Natl Acad Sci U S A* 2006;103(52):19925-19930.
33. Soderling SH, Beavo JA. Regulation of camp and cgmp signaling: New phosphodiesterases and new functions. *Curr Opin Cell Biol* 2000;12(2):174-179.
34. Francis SH, Sekhar KR, Ke H, Corbin JD. Inhibition of cyclic nucleotide phosphodiesterases by methylxanthines and related compounds. *Handb Exp Pharmacol* 2011(200):93-133.
35. van Aubel RA, Smeets PH, Peters JG, Bindels RJ, Russel FG. The mrp4/abcc4 gene encodes a novel apical organic anion transporter in human kidney proximal tubules: Putative efflux pump for urinary camp and cgmp. *J Am Soc Nephrol* 2002;13(3):595-603.
36. Tewson PH, Martinka S, Shaner NC, Hughes TE, Quinn AM. New dag and camp sensors optimized for live-cell assays in automated laboratories. *J Biomol Screen* 2016;21(3):298-305.
37. Vang AG, Ben-Sasson SZ, Dong H, Kream B, DeNinno MP, Claffey MM, Housley W, Clark RB, Epstein PM, Brocke S. Pde8 regulates rapid teff cell adhesion and proliferation independent of icer. *PLoS One* 2010;5(8):e12011.
38. Emery AC, Eiden MV, Eiden LE. A new site and mechanism of action for the widely used adenylate cyclase inhibitor sq22,536. *Mol Pharmacol* 2013;83(1):95-105.
39. Bergeron A, Guillemette C, Sirard MA, Richard FJ. Active 3'-5' cyclic nucleotide phosphodiesterases are present in detergent-resistant membranes of mural granulosa cells. *Reprod Fertil Dev* 2016.
40. Kassel KM, Wyatt TA, Panettieri RA, Jr., Toews ML. Inhibition of human airway smooth muscle cell proliferation by beta 2-adrenergic receptors and camp is pka independent: Evidence for epac involvement. *Am J Physiol Lung Cell Mol Physiol* 2008;294(1):L131-138.
41. Tsai LC, Beavo JA. Regulation of adrenal steroidogenesis by the high-affinity phosphodiesterase 8 family. *Horm Metab Res* 2012;44(10):790-794.
42. Tsai LC, Shimizu-Albergine M, Beavo JA. The high-affinity camp-specific phosphodiesterase 8b controls steroidogenesis in the mouse adrenal gland. *Mol Pharmacol* 2011;79(4):639-648.
43. Shimizu-Albergine M, Tsai LC, Patrucco E, Beavo JA. Camp-specific phosphodiesterases 8a and 8b, essential regulators of leydig cell steroidogenesis. *Mol Pharmacol* 2012;81(4):556-566.
44. Dong H, Osmanova V, Epstein PM, Brocke S. Phosphodiesterase 8 (pde8) regulates chemotaxis of activated lymphocytes. *Biochem Biophys Res Commun* 2006;345(2):713-719.
45. Dong H, Claffey KP, Brocke S, Epstein PM. Inhibition of breast cancer cell migration by activation of camp signaling. *Breast Cancer Res Treat* 2015;152(1):17-28.
46. Dessauer CW, Watts VJ, Ostrom RS, Conti M, Dove S, Seifert R. International union of basic and clinical pharmacology. Ci. Structures and small molecule modulators of mammalian adenylyl cyclases. *Pharmacol Rev* 2017;69(2):93-139.
47. Ostrom RS, Insel PA. The evolving role of lipid rafts and caveolae in g protein-coupled receptor signaling: Implications for molecular pharmacology. *Br J Pharmacol* 2004;143(2):235-245.

AJRCMB Articles in Press. Published on 20-December-2017 as 10.1165/rcmb.2017-0294OC

48. Brown KM, Day JP, Huston E, Zimmermann B, Hampel K, Christian F, Romano D, Terhzaz S, Lee LC, Willis MJ, et al. Phosphodiesterase-8a binds to and regulates raf-1 kinase. *Proc Natl Acad Sci U S A* 2013;110(16):E1533-1542.
49. Cao L, Zhang Y, Cao YX, Edvinsson L, Xu CB. Secondhand smoke exposure causes bronchial hyperreactivity via transcriptionally upregulated endothelin and 5-hydroxytryptamine 2a receptors. *PLoS One* 2012;7(8):e44170.
50. Franciosi LG, Diamant Z, Banner KH, Zuiker R, Morelli N, Kamerling IM, de Kam ML, Burggraaf J, Cohen AF, Cazzola M, et al. Efficacy and safety of rpl554, a dual pde3 and pde4 inhibitor, in healthy volunteers and in patients with asthma or chronic obstructive pulmonary disease: Findings from four clinical trials. *Lancet Respir Med* 2013;1(9):714-727.
51. Wedzicha JA. Dual pde 3/4 inhibition: A novel approach to airway disease? *Lancet Respir Med* 2013;1(9):669-670.
52. Choi YH, Park S, Hockman S, Zmuda-Trzebiatowska E, Svennelid F, Haluzik M, Gavrilova O, Ahmad F, Pepin L, Napolitano M, et al. Alterations in regulation of energy homeostasis in cyclic nucleotide phosphodiesterase 3b-null mice. *J Clin Invest* 2006;116(12):3240-3251.
53. Penn RB, Benovic JL. Regulation of heterotrimeric g protein signaling in airway smooth muscle. *Proc Am Thorac Soc* 2008;5(1):47-57.

Footnotes

** R Development Core Team. R: A Language and Environment for Statistical Computing.* Vienna, Austria: R Foundation for Statistical Computing; 2017.

This work was supported by the National Institutes of Health National Institute of General Medical Sciences [Grant GM107094].

AJRCMB Articles in Press. Published on 20-December-2017 as 10.1165/rcmb.2017-0294OC

Table 1: PDE genes expressed in HASM cells derived from asthma (n=5) and non-asthma (n=10) donors. The mean number of observed reads across all samples and its variance are shown for the most abundant transcript of the corresponding PDE gene. Also shown for these transcripts are the mean and standard deviation of the transcripts per million (TPM), a normalized estimate of transcript expression obtained with kallisto. Six PDE genes (PDE1B, PDE2A, PDE6A, PDE6C, PDE6G, PDE6H) were not expressed (i.e., did not have at least 47% of samples with 5 or more observed reads).

		Observed Reads	**Transcripts per Million (TPM)**
Gene	**Transcript**	Mean (Variance)	Mean (SD)
PDE1A	ENST00000351439	6.00 (0.32)	8.75 (5.13)
PDE1C	ENST00000396184	5.56 (0.70)	1.63 (1.32)
PDE3A	ENST00000359062	5.24 (0.45)	1.27 (0.93)
PDE3B	ENST00000282096	6.26 (0.22)	3.89 (1.73)
PDE4A	ENST00000380702	7.22 (0.02)	11.96 (1.50)
PDE4B	ENST00000371045	5.12 (0.90)	2.55 (2.30)
PDE4C	ENST00000355502	3.57 (0.25)	0.27 (0.14)
PDE4D	ENST00000546160	5.08 (0.54)	1.05 (0.65)
PDE5A	ENST00000394439	9.18 (0.12)	62.61 (22.49)
PDE6B	ENST00000496514	2.34 (1.30)	0.19 (0.13)
PDE6D	ENST00000287600	6.29 (0.02)	21.61 (2.49)
PDE7A	ENST00000401827	5.89 (0.04)	4.21 (0.77)
PDE7B	ENST00000308191	5.26 (0.08)	1.53 (0.48)
PDE8A	ENST00000310298	5.92 (0.16)	4.18 (1.57)
PDE8B	ENST00000264917	4.28 (0.16)	0.54 (0.23)
PDE9A	ENST00000335512	1.45 (2.86)	0.25 (0.29)
PDE10A	ENST00000366882	3.48 (2.25)	0.30 (0.29)
PDE11A	ENST00000286063	1.55 (1.62)	0.03 (0.03)

Figure Legends

Figure 1: Boxplots of transcripts per million (TPM) for the most highly expressed transcript of each PDE gene that had mean observed counts >5, obtained from RNA-Seq results of HASM cells derived from age- and gender-matched fatal asthma (n=5) and non-asthma (n=10) donors. Transcript count estimates were obtained with kallisto using the hg38 Ensembl human genome as reference.

Figure 2: The effect of 30 μM dipyridamole on cAMP accumulation in HASM cells in (A) basal or (B) 1 μM forskolin-stimulated conditions. HASM cells were incubated with recombinant adenoviruses expressing either lacZ, AC2 or AC6 for 18 h. cAMP accumulation was then measured over 10 min in the presence of 200 μM IBMX. Data is expressed as the mean ± S.E.M. of n=5. * denotes $p < 0.05$ by paired t-test as compared to vehicle.

Figure 3: PDE8A knockdown in HASM cells. (A) Immunoblot analysis of PDE8A and ß-actin in HASM cells after 72 h incubation with recombinant lentivirus expressing scrambled or PDE8A shRNA. The PDE8A antibody detected multiple non-specific bands. The genuine PDE8A immunoreactivity was identified based on the expected molecular weight of 93 kDa so only this band is shown (representative images of n=3 are shown). Full immunoblot of PDE8A is shown in supplementary data Figure S1. (B) Immunoreactive bands were analyzed by densitometry using volume plus density and PDE8A density was normalized to the ß-actin loading control. Data is expressed as the mean ± S.E.M. of n=3. ** denotes $p < 0.01$ by paired t-test as compared to control. The effect of PDE8A knockdown on cAMP accumulation in HASM cells in basal (C) or 1 μM forskolin-stimulated (D) conditions. HASM cells were incubated with recombinant lentivirus expressing scrambled or PDE8A shRNA for 72 h, and recombinant adenoviruses expressing either lacZ, AC2 or AC6 for 18 h. cAMP accumulation was measured over 10 min in the presence of 200 μM IBMX. Data is expressed as the mean ± S.E.M. of n=5.

AJRCMB Articles in Press. Published on 20-December-2017 as 10.1165/rcmb.2017-0294OC

* denotes $p < 0.05$ by paired t-test as compared to lacZ, # denotes $p < 0.05$ by paired t-test as compared to control. cAMP stimulated by various concentrations of forskolin were measured in HASM cells overexpressing either AC2 (E) or AC6 (F). Data is expressed as the mean ± S.E.M. of n=4. Nonlinear regression analysis was used to fit each data set. The $pLog_{EC50}$ for forskolin in AC6 cells was -4.97 ± 0.232 and the E_{max} value was 4.96 ± 0.785. The $pLog_{EC50}$ for forskolin in AC6 cells treated with PDE8A shRNA was -6.24 ± 0.481) and the E_{max} value was 9.069 +/- 0.609.

Figure 4: cAMP dynamics in live HASM cells measured using the cADDis assay. HASM cells were incubated with recombinant BacMam virus expressing the cADDis cAMP sensor for 24 h. After establishing baseline, fluorescence decay was monitored for 30 min after addition of the indicated agent. cADDis sensor fluorescent decay curves elicited by various concentrations of forskolin (A), PF-04957325 (B) or rolipram (C) are shown, with each point representing the mean ± S.E.M. of n = 3-5. Responses to the same concentrations of PF-04957325 were measured in the presence of 10 μM SQ22536 to reduce basal cAMP synthesis (D). The ability of SQ22536 to inhibit adenylyl cyclase activity was confirmed in HASM membranes stimulated with 1 μM forskolin or forskolin plus 10 μM SQ22536 (D, inset). PF-04957325 was tested at concentrations from 10^{-11} M (lightest filled circle) to 10^{-6} M (black filled circle). Control (vehicle) responses are plotted as dotted open circles, 10 μM forskolin plotted as dotted open squares. Data are gathered as arbitrary fluorescence units and expressed as observed fluorescence (F) over initial fluorescence (F_0) to indicate remaining fluorescence after stimulation. 10 μM SQ22536 was added 5 minutes prior to initiating 30 minute read with PF-04957325. Kinetic rate constants (k) were derived from a shared constrained plateau of one-phase decay analysis among the control and the doses of PF-04957325 with constrained Hill slope = 2 and plotted (E). The $pLog_{EC50}$ for PF-04957325 alone was determined to be -8.034 ± 0.193 and the E_{max} value for the span of k was 0.00516 ± 0.00118. The $pLog_{EC50}$ for PF-04957325 with 10 μM

SQ22536 was determined to be -6.921 ± 0.339 and the E_{max} value for the span of k was 0.001341 ± 0.0005293. Each bar represents the mean ± S.E.M. of n = 5. * denotes $p < 0.05$ by paired t-test as compared to control.

Figure 5: Dose response of the selective PDE8 inhibitor, PF-04957325, on isoproterenol- or PGE_2-stimulated cAMP dynamics in live HASM cells. Representative cADDis sensor fluorescent decay curves (F/F_0) are shown for minimally effective concentrations of isoproterenol (1 nM) or PGE2 (3 nM) with and without 10 μM SQ22536 to suppress basal AC activity (A). Various concentrations of PF-04957325 were then added to these same conditions. Representative decay curves are shown in the presence of 10 μM SQ22536 plus either 1 nM isoproterenol (B) or 3 nM PGE2 (C). PF-04957325 was tested at concentrations from 10^{-11} M (lightest circle) to 10^{-6} M (black circle). Kinetic rate constants (k) from one-phase decay analysis (with a shared constrained plateau) were calculated for each dose of PF-04957325 and the pooled data from multiple experiments is shown (D). Each bar represents the mean ± S.E.M. of n=5. * denotes $p < 0.05$ by paired t-test as compared to isoproterenol.

Figure 6: Western blot analysis of PDE8A in fractions from sucrose density centrifugation from control HASM cells or cells incubated 72 h with recombinant lentivirus expressing PDE8A shRNA. Cells were fractionated using a non-detergent method and separated by sucrose density centrifugation (see *Materials and Methods*). Gradients were collected in ten, 0.5 mL fractions and separated by SDS-PAGE and analyzed by immunoblotting using a primary antibody for PDE8A. Fractions were also probed for native expression of AC6, AC2 and caveolin-1 using antibodies for AC5/6. AC2 and caveolin-1 to show appropriate fractionation (both control and PDE8A knockdown HASM cells displayed similar distribution of both caveolin-1, AC5/6 and AC2). Fractions 3-5 contain with buoyant, lipid raft membranes while fractions 6-10 contain the rest of the cellular material. Shown are regions of the gels at the approximate

AJRCMB Articles in Press. Published on 20-December-2017 as 10.1165/rcmb.2017-0294OC

molecular weight of the expected immunoreactive band. Images shown are representative of 3 experiments.

Figure 7: Cell proliferation was measured using CyQUANT NF in HASM cells stimulated with 10% FBS for 48 h. 1 μM isoproterenol (A) or PGE2 (B) were included with and without addition of 1 μM PF-04957325 in both serum free and 10% FBS conditions. The data is normalized to the serum-free basal condition and expressed as fold over basal. Each bar represents the mean ± S.E.M. of n=4-7. # denotes $p<0.05$ as compared to serum free basal. * denotes $p<0.05$ and ** denotes $p<0.01$ compared to 10% FBS alone by paired t-test.

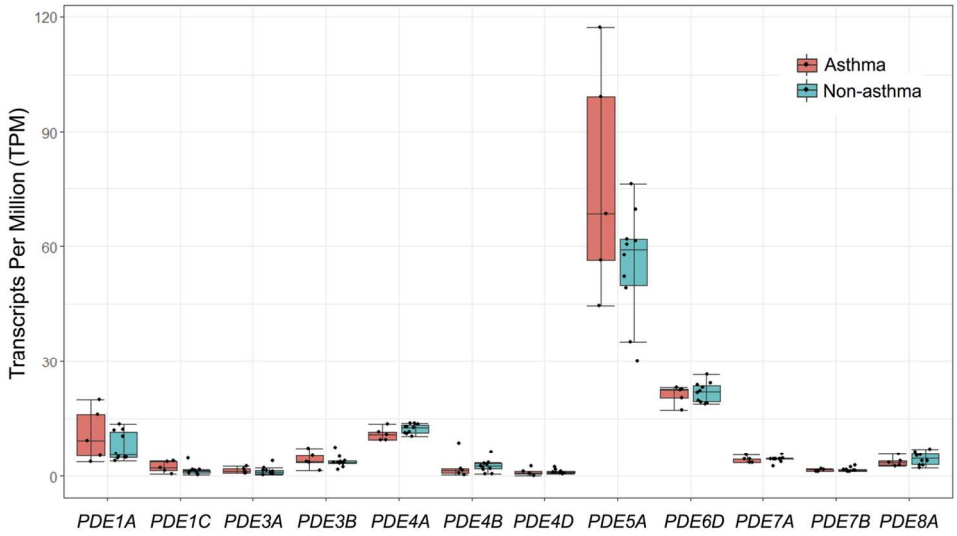

Figure 1

132x75mm (300 x 300 DPI)

AJRCMB Articles in Press. Published on 20-December-2017 as 10.1165/rcmb.2017-0294OC

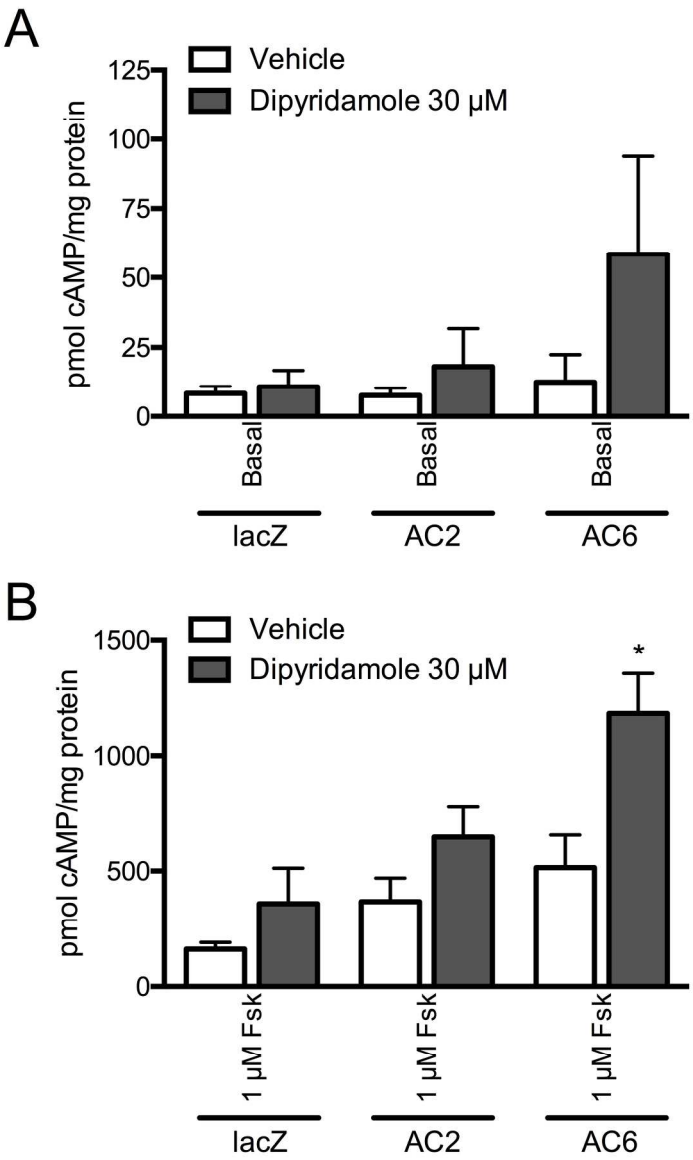

Figure 2

162x267mm (300 x 300 DPI)

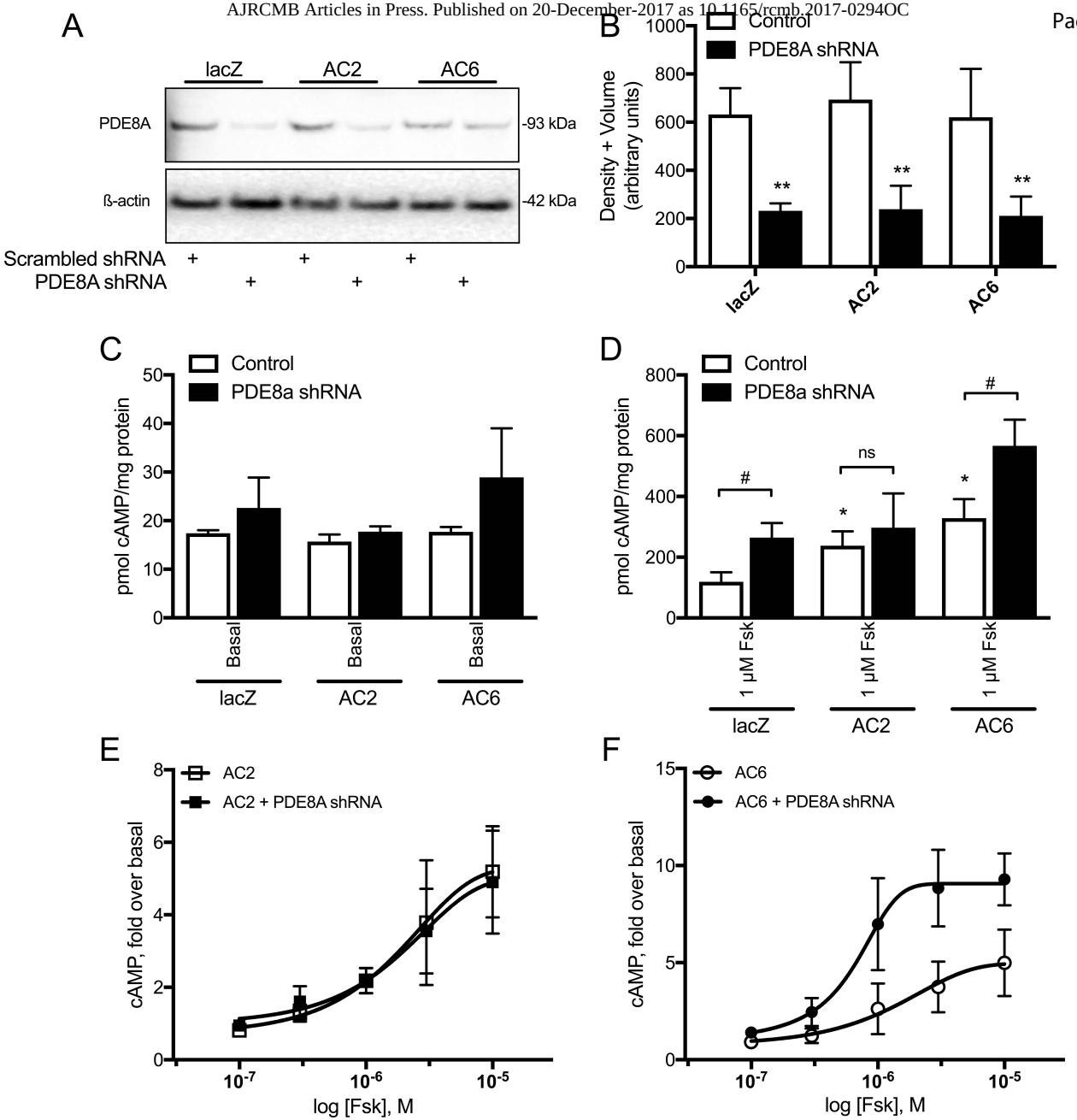

Figure 3

AJRCMB Articles in Press. Published on 20-December-2017 as 10.1165/rcmb.2017-0294OC

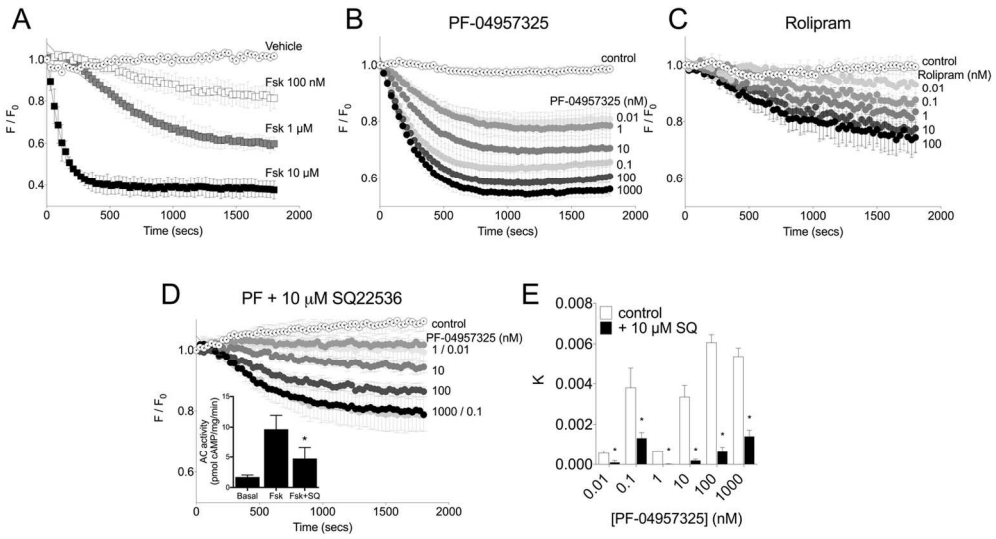

Figure 4

135x74mm (300 x 300 DPI)

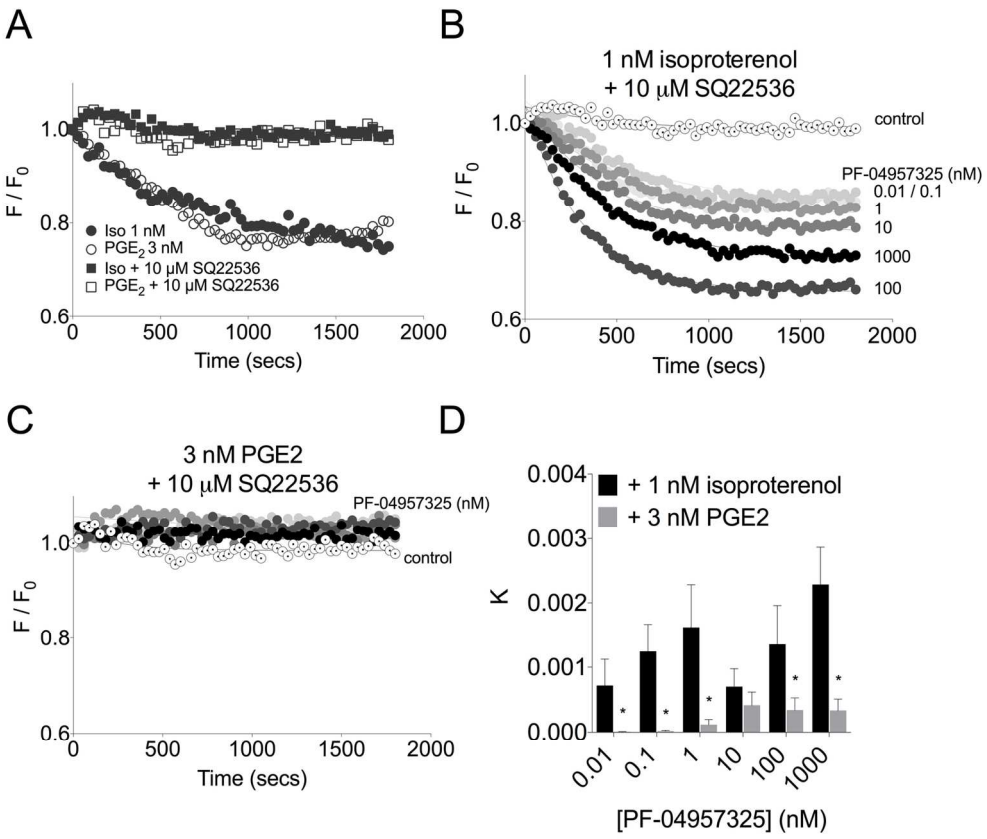

Figure 5

150x128mm (300 x 300 DPI)

AJRCMB Articles in Press. Published on 20-December-2017 as 10.1165/rcmb.2017-0294OC

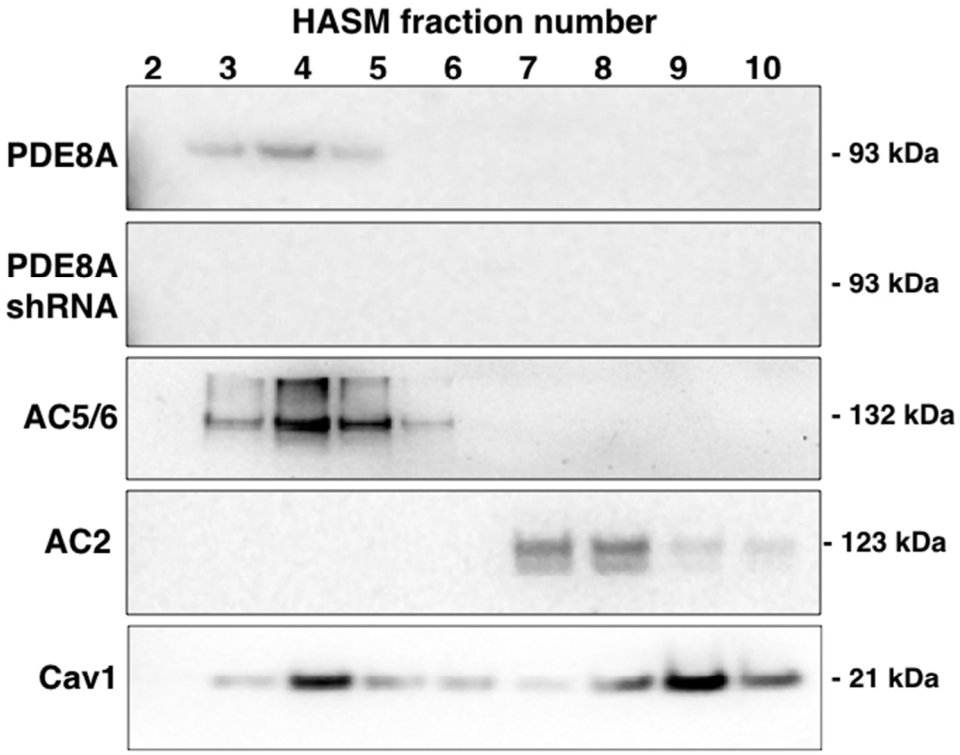

Figure 6

251x200mm (72 x 72 DPI)

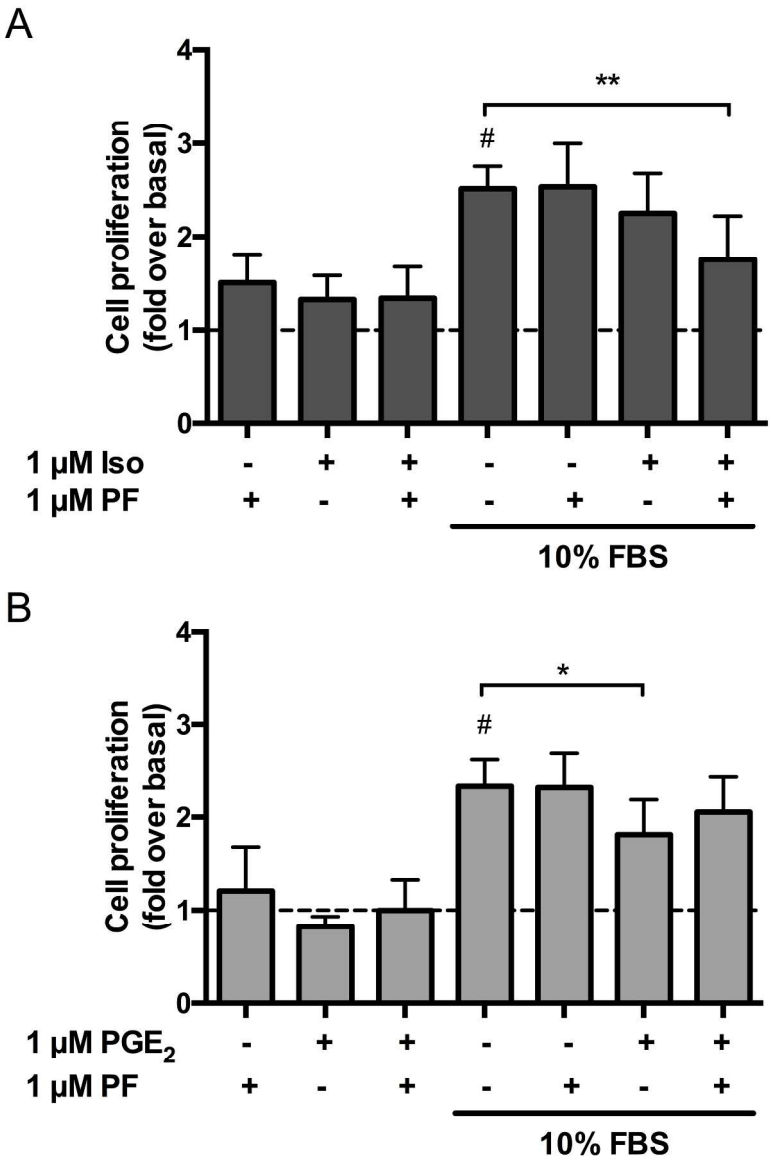

Figure 7

205x311mm (300 x 300 DPI)

AJRCMB Articles in Press. Published on 20-December-2017 as 10.1165/rcmb.2017-0294OC

Online data supplement

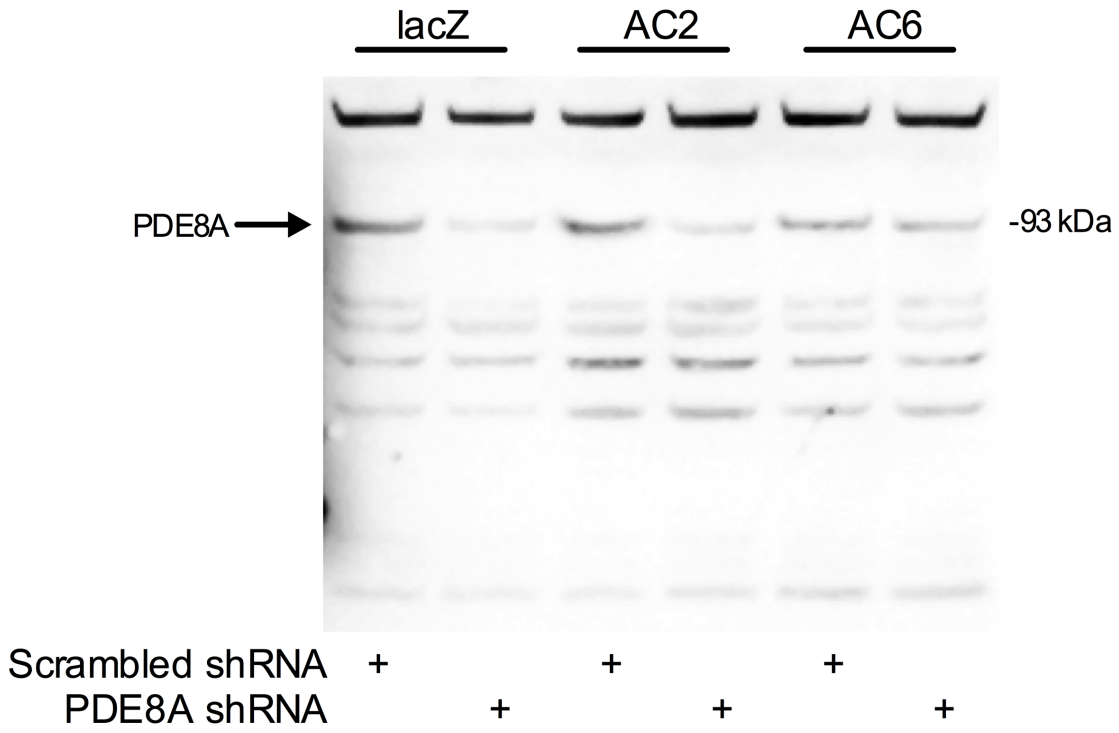

Figure S1: Immunoblot analysis of PDE8A in HASM cells after 72 h incubation with recombinant lentivirus expressing either scrambled or PDE8A shRNA. The PDE8A antibody used detected multiple non-specific bands so the whole blot is shown. The genuine PDE8A immunoreactivity was identified based on the expected molecular weight of 93 kDa. HASM were also incubated with recombinant adenoviruses expressing either lacZ, AC2 or AC6 for 18 h.

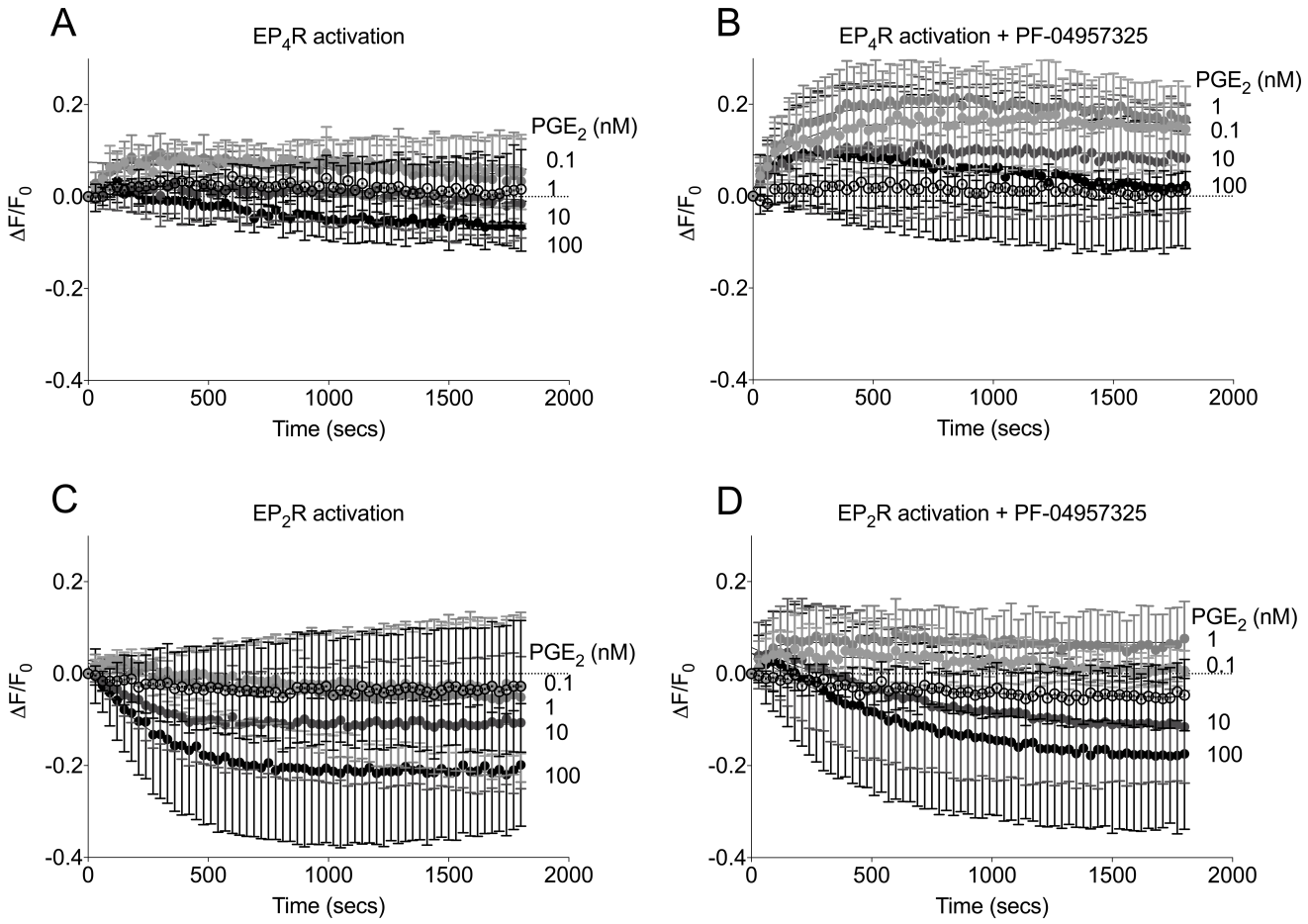

Figure S2: cAMP dynamics in live HASM cells measured using the cADDis assay. HASM cells were incubated with recombinant BacMam virus expressing the cADDis cAMP sensor for 24 h. Fluorescence decay was monitored for 30 min after addition of various concentrations of PGE_2 in the presence of either 100 nM PF-044118948 (EP_2R-selective antagonist, panel A), 100 nM PF-044118948 plus 1 μM PF-04957325 (panel B), 300 nM GW-627368X (EP_4R-selective antagonist, panel C) or 300 nM GW-627368X plus PF-04957325 (D). Open symbols show the vehicle control, which contained the indicated antagonist and inhibitor, but no PGE_2. Each point represents the mean ± S.E.M. of n = 5-6. No statistically significant differences exist in either response upon treatment with PF-04957325 (one way ANOVA).